NASA Technical Memorandum 82993

Initial Stages of Cavitation Damage and Erosion on Copper and Brass Tested in a Rotating Disk Device

P. Veerabhadra Rao and B. C. Syamala Rao
Lewis Research Center
Cleveland, Ohio

and

N. S. Lakshmana Rao
Indian Institute of Science
Bangalore 560012, India

Prepared for the
Cavitation and Polyphase Flow Forum
sponsored by the American Society of Mechanical Engineers
St. Louis, Missouri, June 7-11, 1982

NASA

THE INITIAL STAGES OF CAVITATION DAMAGE AND EROSION ON COPPER AND BRASS TESTED IN A ROTATING DISK DEVICE

P. Veerabhadra Rao[1] and B. C. Syamala Rao[1]
National Aeronautics and Space Administration
Lewis Research Center
Cleveland, Ohio 44135

and

N. S. Lakshmana Rao
Indian Institute of Science
Department of Civil Engineering
Bangalore 560012, India

SUMMARY

Microphotographs showing the mechanism of cavitation damage during incubation periods on polycrystalline copper and brass tested in a rotating disk device are presented. The similarities and differences in the damage mechanism in a rotating disk device (which simulates field rotary devices) and in a magnetostriction apparatus are discussed. The macroscopic erosion appears similar to that in a vibratory device except for nonuniform erosion and apparent plastic flow during the initial damage phases.

E-1424

INTRODUCTION

In order to study the microstructural effects of cavitation erosion of different materials in relatively short times, the magnetostriction apparatus has been used by numerous investigators (e.g., refs. 1 to 5). This is primarily due to its relatively low cost and versatility in producing highly accelerated cavitation damage. However, ultrasonic vibrators produce deformation different from that in most flow devices due to the following facts: (a) severe damage in a short time; (b) possible increase of the mechanical aspect of erosion relative to corrosion and other influences; and (c) synchronized cavity collapse. In view of these differences there has been a continuing debate as to whether or not the vibratory cavitation damage produced in an ultrasonic device is similar to the damage occurring in cavitating flow systems (i.e., in venturi and rotating disk devices). Several investigators used both venturi (refs. 3 to 10) and rotating disk (ref. 7) devices for obtaining cavitation damage on different materials and studying variations in their metallurgical properties. Many of the earlier investigations were concerned with erosion during its advanced stages. However, it is only recently that the mechanism during the initial phases of erosion, viz., "incubation period" has attracted a few investigators (e.g., refs. 2 to 4). The main objectives of these research efforts were to understand clearly the influence of metallurgical parameters on the initiation of erosion damage as well as to aid in the development of new erosion resistant materials. Some studies concentrated on erosion mechanisms similar to those between the venturi and vibratory cavitation devices and between cavitation and liquid impact (refs. 3, 4, 12).

---

[1]NRC - NASA Research Associates.

The present study concerns itself with the mechanism of erosion during the incubation period[2] on polycrystalline copper and brass specimens tested in a rotating disk device.

EXPERIMENTAL DEVICE AND TEST CONDITIONS

The rotating disk device, Fig. 1(a), consists of a cast iron chamber in which a metallic disk of 330 mm diameter rotates (ref. 13). The chamber is provided with eight radial baffles spaced at equiangular distances on either side of the disk to prevent overall circulation of water contained in the chamber. The chamber is connected to an overhead tank for the supply of water. The inlet and outlet valves provided for the chamber are used for regulating pressure and temperature in the chamber. The rotating disk, figure 1(b), consists of a 1.5 mm thick mild steel base sheet covered by a 3 mm thick aluminum sheet. Six diametrically opposite grooves of 64 mm diameter are cut in the latter to fix test specimens of 63.5 mm diameter. Polycrystalline copper and brass were tested using water. The mechanical and other properties of these two materials are presented in table 1. The experimental conditions were as follows: velocity, 35 to 37.3 m/s; pressure, 0.15 MPa (abs); temperature, 34 ± 2^{o} C; diameter and height of the yellow brass cavitation inducer, 25.4 and 3 mm, respectively; and the diameter and thickness of specimens - 63.5 and 3 mm, respectively. The copper and brass specimens were etched with potassium dichromate and photographed before being exposed to cavitation.

RESULTS AND DISCUSSION

Figures 2(a) and 3(a) showing the specimen surfaces before test, indicate slight artifacts resulting from sample preparation and etching. During the first 20 to 30 seconds of cavitation attack at a velocity of 37.3 m/sec, damage is seen at the grain boundaries and coarse slip bands develop across the grains on copper (fig. 2(b)). Pits of varying size (~ 5 to 25 μm) and shape appear randomly on the surface. The incubation periods (during which no measurable weight losses were observed) for copper and brass are presented in Table 2 for erosion at different velocities.

With increased cavitation attack, the reflectivity of the surface gradually reduced, indicating an increase of pit size and number. The formation of the pits or craters does not appear to be associated with the grain boundaries or other structural/metallurgical features except the etch pits resulting from sample preparation. Using a magnetostriction oscillator, Vyas and Preece (ref. 2) observed similar trends on face centered cubic (fcc) metals like nickel, copper, and aluminum. However, in the present investigation, there seems to be evidence showing that the deformation starts at inclusions and at unfavorably oriented grains and transforms into pits (figs. 2(b) to (d) and (h)). Slip lines are seen around the pit. As the exposure increases from 1 to 3.5 min, the pits gradually broaden across grains as seen from figures 2(d) to (f). The straddling of grain boundaries may be due to differing amounts of plastic deformation within each grain. The central portion of the pits is not damaged initially, indicating a possible type of microjet and/or shockwave

---

[2]Some investigators define "incubation period" as the no weight loss period. While other investigators define it as the intercept on the time axis obtained by extending the straight line portion of the cumulative erosion-time curve. The present investigations are concerned with the mechanism of damage occurring during the former period.

attack. This type of central undamaged attack is not reported with the magnetostriction and other flow-type devices. During the initial stages, the depth of an individual pit is much less than its surface dimension/area. Because several pits appear on a single grain and the eroded particles are smaller compared to the grain size, grains are believed to be breaking up.

During the initial stages of plastic deformation, there is little indication of the opening up of the grain boundaries to develop into cracks, although the photograph in figure 2(g) is indicative of this possibility. As the exposure increases, the deformed depressions turn into pits, suggesting the development of plastic deformation into fracture due to stress concentration caused by an unfavorable surface configuration. It may be possible that soft regions of lower average yield stress or very small rough regions on the surface could account for local yielding due to impact even though the average impact pressure is low.

The slip lines are initially arrested by grain boundaries, although transcrystalline damage is observed at severely pitted areas. With further exposure to cavitation, the deformation is primarily by pit formation (fig. 2(h)). The grain structure is completely destroyed and a lot of material flow is observed after 10 min (fig. 2(k)). The particle-removal is believed to occur by ductile tearing from the craters by the end of the incubation period (fig. 2(k)). The macroscopic ductile flow of material is seen in figure 2(l). The "tunnelling effect" observed for both vibratory cavitation and liquid-impingement erosion devices (ref. 12) and on stainless steel using a rotating disk device (ref. 14) is not observed in the present investigation.

A series of photographs taken during the incubation period of a brass specimen is shown in figure 3. Brass has more microscopic pits than copper (fig. 2). The α and β phase boundaries are believed to provide suitable sites for deformation. Deformed material can be seen at the pit bottom (fig. 3(e)) and at the pit rim (fig. 3(f)). The overall pit size is almost the same as on copper, except that on brass each macropit occupies several grains. The progress of damage and erosion initiation are found to be almost similar to those on copper.

Figures 4 and 5 present SEM micrographs of eroded area on brass. Figure 4(a) presents an overall view of the eroded region, depicting large craters and subsurface cracking. Figure 4(b) presents a magnified view of the area A shown in figure 4(a). Two large craters with the flow of material around the rim may be seen in the figure. Figure 4(c) presents a surface profile along a-a shown in figure 4(a). The large peak indicates the flow of material around the rim of a crater/pit of largely eroded area. Figures 4(d) and (e) present high magnification views of the areas B and C, respectively, depicted in figure 4(b). The irregular shape of the craters and the flow of material around the rim may clearly be seen in these figures. Figures 5(a) and (b) also present magnified views of a single irregular, relatively shallow crater of approximately 120 μm size. The flow of material along the rim may once again be seen in detail in these figures.

Figures 6(a), (b), and (c) present surface profiles of the eroded area. Figure 6(a) is a surface profile in the lightly eroded area, while figure 6(b) is in a highly eroded area. The individual pits are of the size 30 to 50 μm, while the craters are as big as 0.25 to 0.5 mm in size. The depth of individual pits is around 20 to 50 μm.

MICROHARDNESS CHANGE

Microhardness traverses taken over a damaged area of 20 by 20 mm on copper indicates an increase of 32 percent. This type of work-hardening phenomenon is also observed on the back of the specimen exactly behind the gross damage/ erosion spot (ref. 14). The present investigation also indicates a reduction in microhardness just prior to the end of the incubation period. This may possibly be attributed to fatigue-softening which is generally believed to decrease the yield strength and to increase local ductility. The observation of more plastic flow during the initial phases in the present investigation (figs. 2 and 3) and in an earlier study of the authors (ref. 13) may be related to this fatigue-softening effect. Further studies are necessary to understand more about this phenomenon.

CONCLUDING REMARKS

The studies conducted so far on copper and brass using a rotating disk and by others using a magnetostriction oscillator (e.g., refs. 1, 2) and a double weir arrangement (refs. 6, 7) reveal several similarities, as well as differences in the mechanism/ process of damage and erosion as follows:

Similarities. - (a) The formation of pits and craters is not related to any structural/ metallurgical feature (except that they initiate at inclusions and unfavorably oriented grains in a rotating disk device). (b) The straddling of grain boundaries and pushing and tilting of grains are observed in both the cases. (c) During the advanced phases of damage (before actual measurable weight loss or the end of incubation period) the deformation is chiefly by crater formation. (d) An increase in microhardness is observed both on the front and back of the specimens. (e) Cracks observed on copper (ref. 1) and on a copper alloy (ref. 6) are also observed in the present investigations at an advanced stage of erosion.

Differences. - (a) The initial phases of erosion in a rotating disk device show more ductile flow and failure than in other types of devices. (b) A decrease in microhardness is observed on copper tested in a rotating disk device. (c) The tunnelling effect, observed on several materials for both vibratory cavitation and liquid impingement erosion processes (ref. 12) and on stainless steel tested in a rotating disk device (ref. 14), is not noticed in the present study.

REFERENCES

1. Vasvari, F., "Investigation of Initial Phase of Cavitation Damage," Acta Technica Academiae Scientiarum Hungaricae, Vol. 39, No. 1-2, 1962, pp. 101-121.

2. Vyas, B., and Preece, C. M., "Cavitation Erosion of Face Centered Cubic Metals," Metallurgical Translations A, Vol. 8A, June 1977, pp. 915-923.

3. Hansson, I., Morch, K. A., and Preece, C. M., "A Comparison of Ultrasonically Generated Cavitation Erosion and Natural Flow Cavitation Erosion," Proc. Ultrasonics International 1977, Z. Novak, ed., IPC Science and Technology Press, 1977 pp. 267-274.

4. Hansson, I., and Morch, K. A., "Comparison of the Initial Stage of Vibratory and Flow Cavitation Erosion," Proc. 5th Conf. on Erosion by Solid and Liquid Impact, Sept. 1979, Cambridge University, England, Paper 60.

5. Hackworth, J. V., and Adler, W. F., "Microscopic Investigation of Cavitation Erosion Damage in Metals," The Role of Cavitation in Mechanical Failures, T. R. Shives and W. A Willard, eds., National Bureau of Standards, Washington, D. C., 1973, pp. 54-59.

6. Boetcher, H. N., "Failure of Metals Due to Cavitation Under Experimental Conditions," ASME Transactions, Vol. 58, No. 5, July 1936, pp. 355-360.

7. Mousson, J. M., "Pitting Resistance of Metals Under Cavitation Conditions," ASME Transactions, Vol. 59, No. 5, July 1937, pp. 399-408.

8. Hammitt, F. G., et al., "Initial Phases of Damage to Test Specimens in a Cavitating Venturi," ASME Journal of Basic Engineering, Vol. 87, No. 2, June 1965, pp. 453-464.

9. Hansson, I., and Morch, K. A., "SEM Studies of Cavitation Erosion," Scandinavian Journal of Metallurgy, Vol. 6, No. 1, 1977 pp. 10-12.

10. Hansson, I., Kristensen, J. K., and Morch, K. A., "A Simple Model for Cavitation Erosion of Metals," Journal of Physics, Ser. D, Applied Physics, Vol. 11, No. 6, Apr. 1978 pp 899-912.

11. Wood, G. M., Knudsen, L. K., and Hammitt, F. G., "Cavitation Damage Studies with Rotating Disk in Water," ASME Journal of Basic Engineering, Vol. 89, No. 1, Mar. 1967, pp. 98-110.

12. Preece, C. M., and Brunton, J. H., "A Comparison of Liquid Impact Erosion and Cavitation Erosion," Wear, Vol. 60, No. 2, May 1980 pp. 269-280.

13. Veerabhadra Rao, P., Syamala Rao, B. C., and Lakshmana Rao, N. S., Erosion and Cavity Char- acteristics in Rotating Components," Journal of Testing and Evaluation, Vol. 8, No. 3, May 1980 pp. 127-142.

14. Veerabhadra Rao, P., "Characteristics, Correlations, Similarities and Prediction of Erosion Due to Cavitation and Liquid Impingement," Ph. D. Thesis, Indian Institute of Science, Bangalore, India, Sept. 1975.

TABLE 1. - MECHANICAL AND OTHER PROPERTIES OF COPPER AND BRASS

Property	Copper	Brass
Density, kg/m^3	8.95×10^3	8.5×10^3
Yield strength, MPa	97.7	108.2
Tensile strength, MPa	180.5	213.9
Elastic modulus, GPa	117.2	110.4
Hardness (Brinell H)	58	150
Strain energy[a], $MN-m/m^3$	65.8	81.8
Ultimate resilience[b], $KN-m/m^3$	139	207
Modified resilience[c]	0.045	0.145
Fracture strength, MPa	115.8	158.4
Elongation, percent	43	46
Reduction in area, percent	48	52

[a]Area under the engineering stress-strain curve.
[b](Tensile strength)^2/(2 x elastic modulus).
[c](Tensile strength x hardness)/(2 x elastic modulus). This property is represented in the units of hardness.

TABLE 2. - INCUBATION PERIOD AND TIME TO ATTAIN PEAK RATE OF EROSION FOR COPPER AND BRASS SPECIMENS (PRESSURE = 0.15 MPa (abs), INDUCER DIAMETER = 25.4 mm).

Material	Velocity, m/sec	Incubation period, min	Peak rate of of erosion, mm^3/min	Time to attain peak rate, min
Copper	37.3	12.5	0.43	90
	36.6	90	---	---
	35.8	210	---	---
	35.0	270	---	---
Brass	37.3	20.5	0.18	300
	36.6	240	0.02	1260
	35.8	270	0.017	1260
	35.0	300	0.007	1260

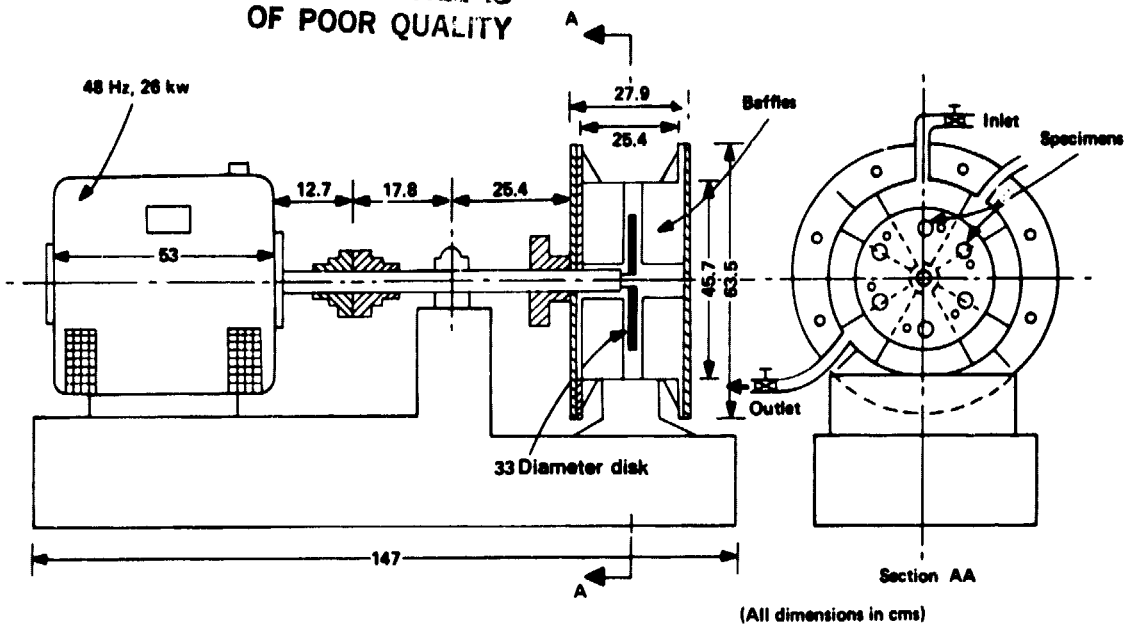

(a) Sectional views of the rotating disk setup.

Figure 1. - Rotating disk device.

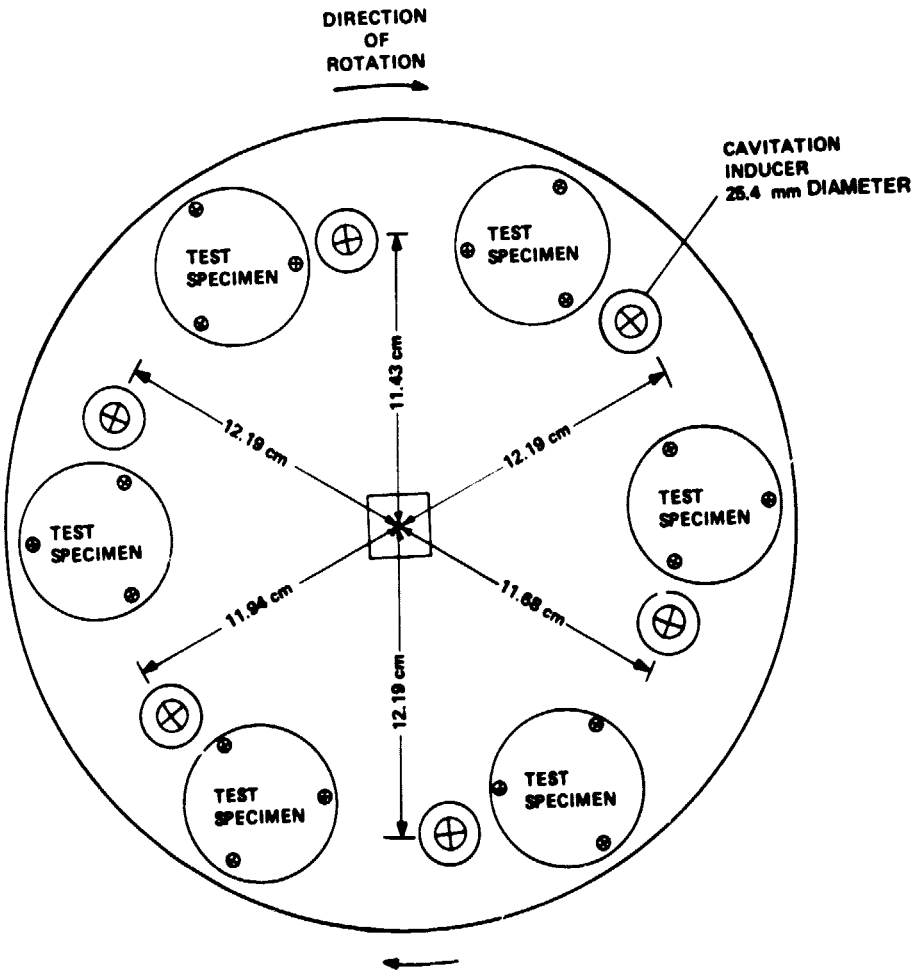

(b) Details of the rotating disk.

Figure 1. - Concluded

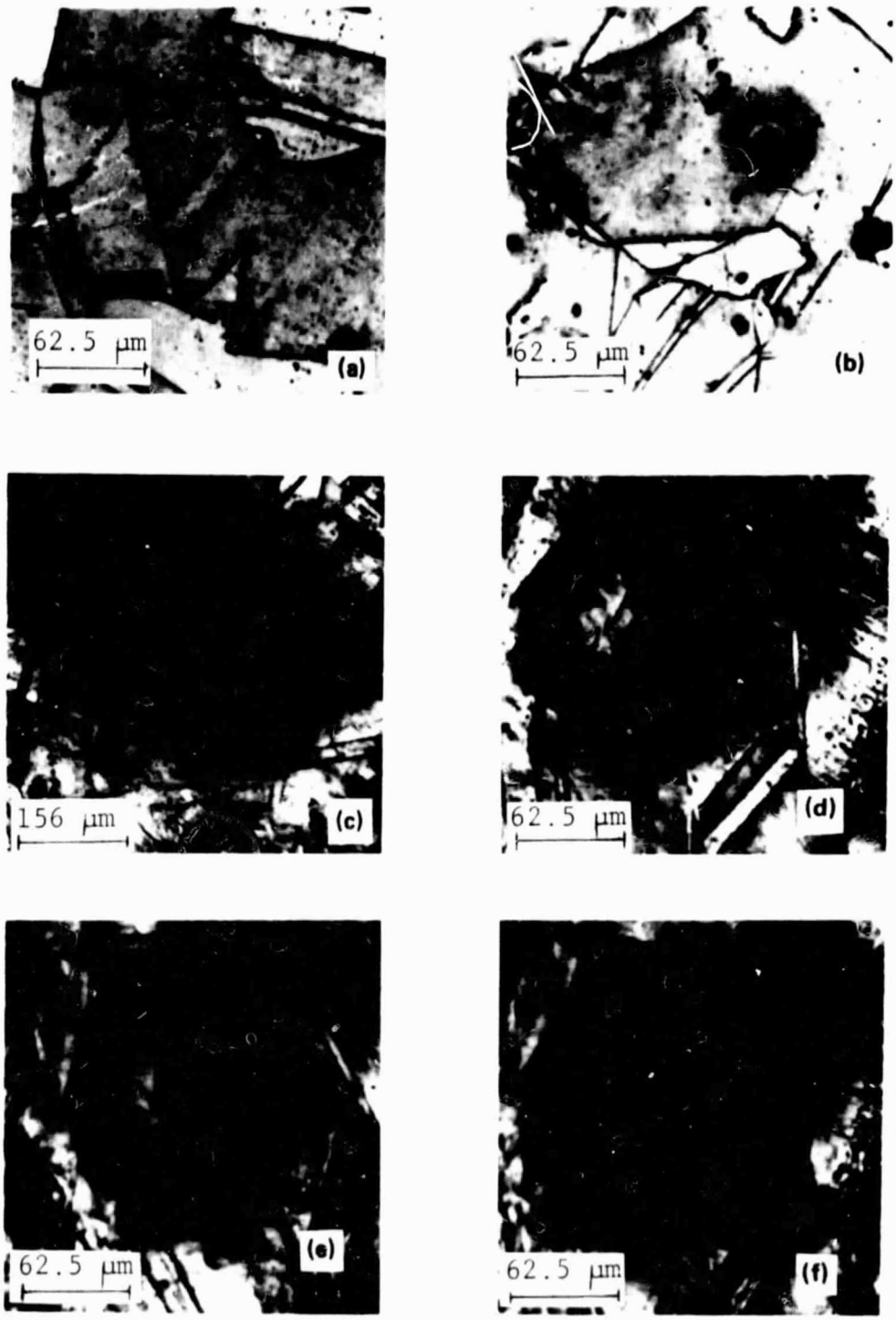

Figure 2. - Photographs of damage progress on copper specimen exposed to cavitation in a rotating disk device at 0.15 MPa (abs) pressure and 37.3 m/s flow velocity. (a) unexposed surface, (b) 0.5 min (damage initiation at weak spots), (c) 1 min, (sliplines and pit formation), (d) 1.5 min, (e) 3 min, (f) 3.5 min.

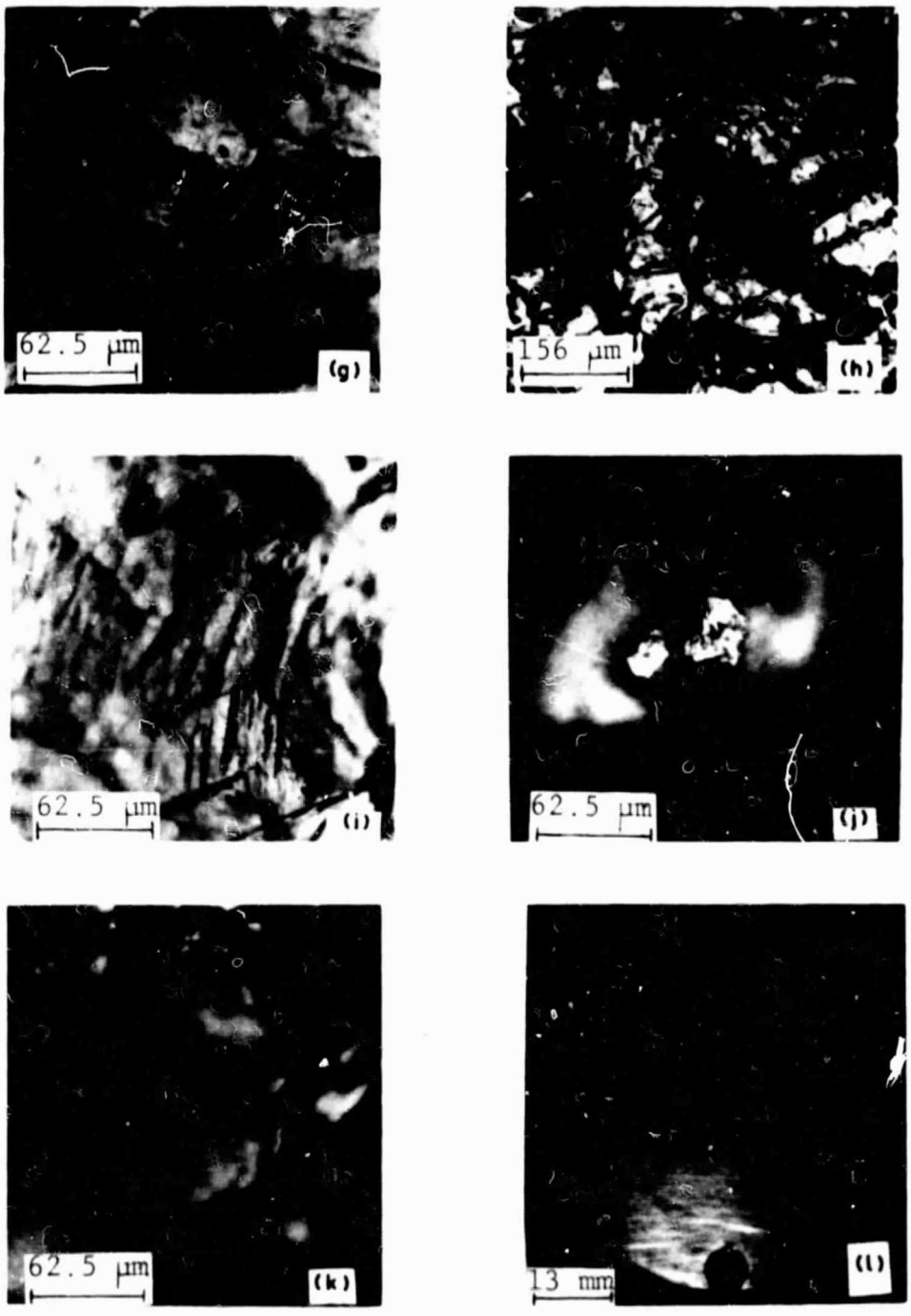

Figure 2. - Concluded. (g) 4 min (damage along grain boundaries and tilting of grains), (h) 4 min (complete grain damage), (i) 5 min (multiple slip), (j) 6 min (pit bottom with plastic flow), (k) 10 min (pits with flow of material), (l) 120 min (macroscopic flow on material surface).

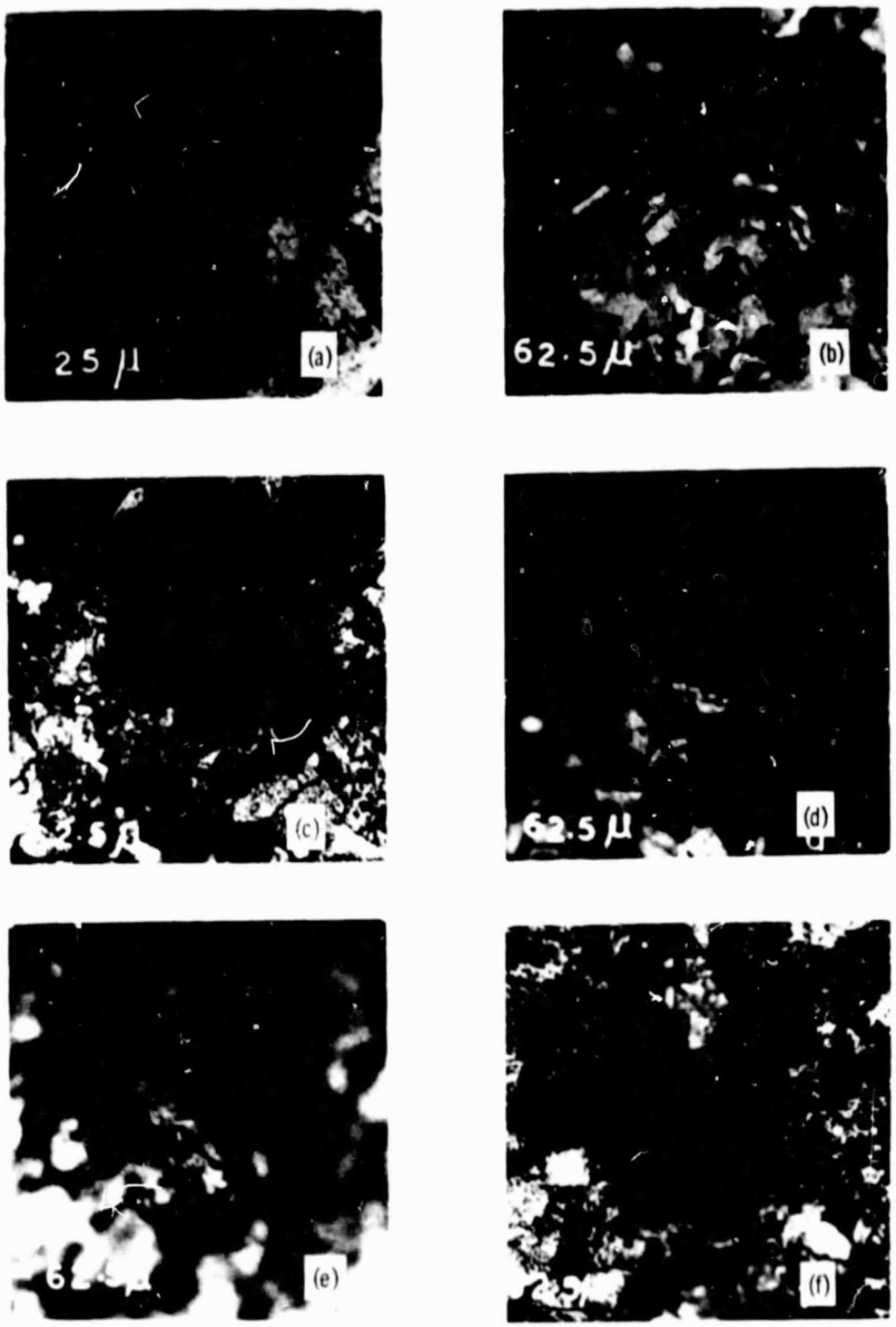

Figure 3. - Photographs of damage progress on brass specimen exposed to cavitation in a rotating disk device at 0.15 MPa (abs) pressure and 37.3 m/s flow velocity. (a) unexposed surface, (b) 3 min (slip lines), (c) 8 min (pit with plastic deformation and flow), (d) 11 min (pit bottom with plastic deformation and flow), (e) 15 min (compietely damaged grain structure), (f) 15 min (pit with flow on the rim).

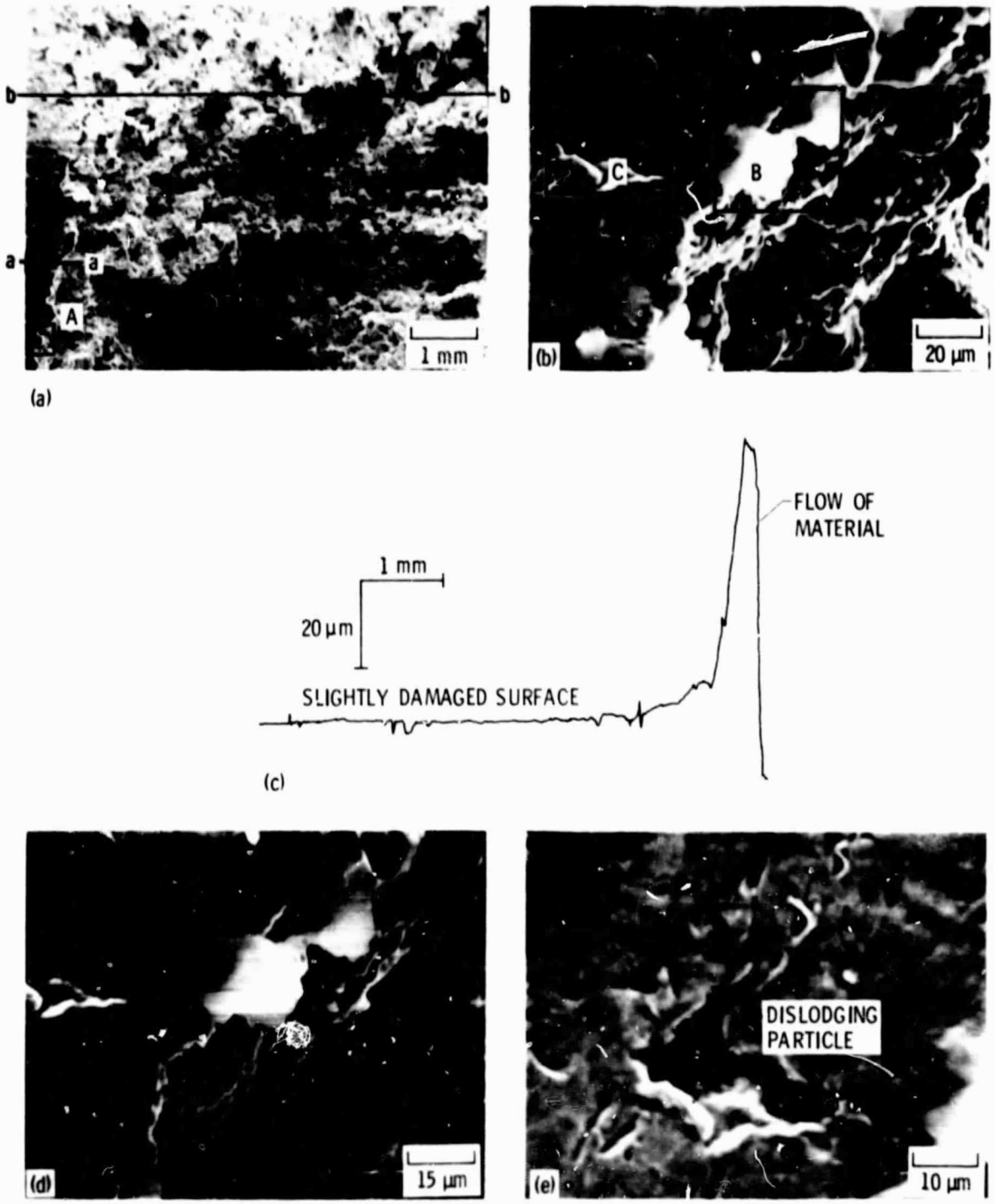

(a) General view of highly eroded region.

(b) High magnification view at area A shown in (a).

(c) Surface profile along a-a in (a) showing flow of material.

(d) High magnification view at B shown in (b).

(e) High magnification view at C shown in (b).

Figure 4. - SEM micrographs of eroded area with flow of material.

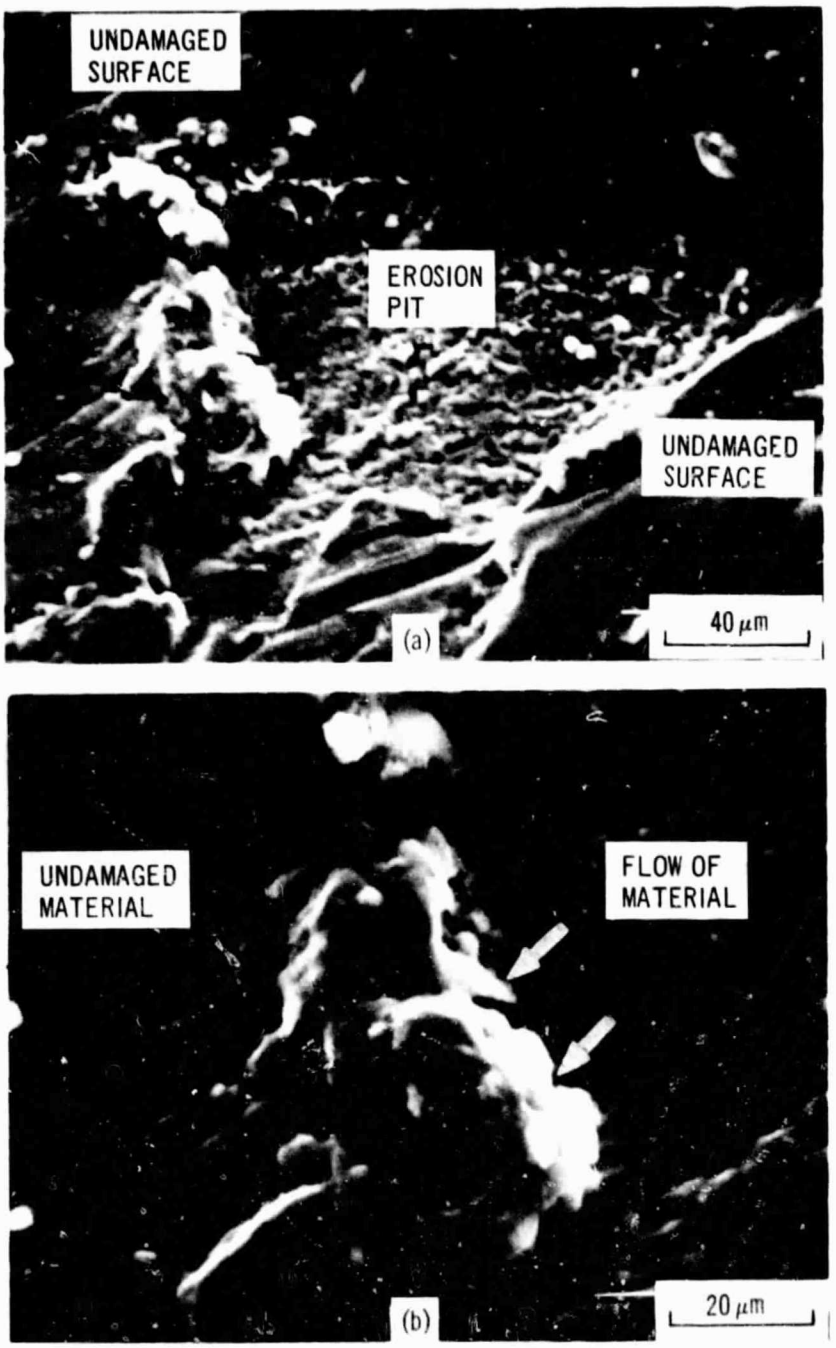

(a) Cavitation erosion pit with debris.

(b) Cavitation erosion pit showing flow of material.

Figure 5. - Single eroded pit on brass showing flow of material on the rims.

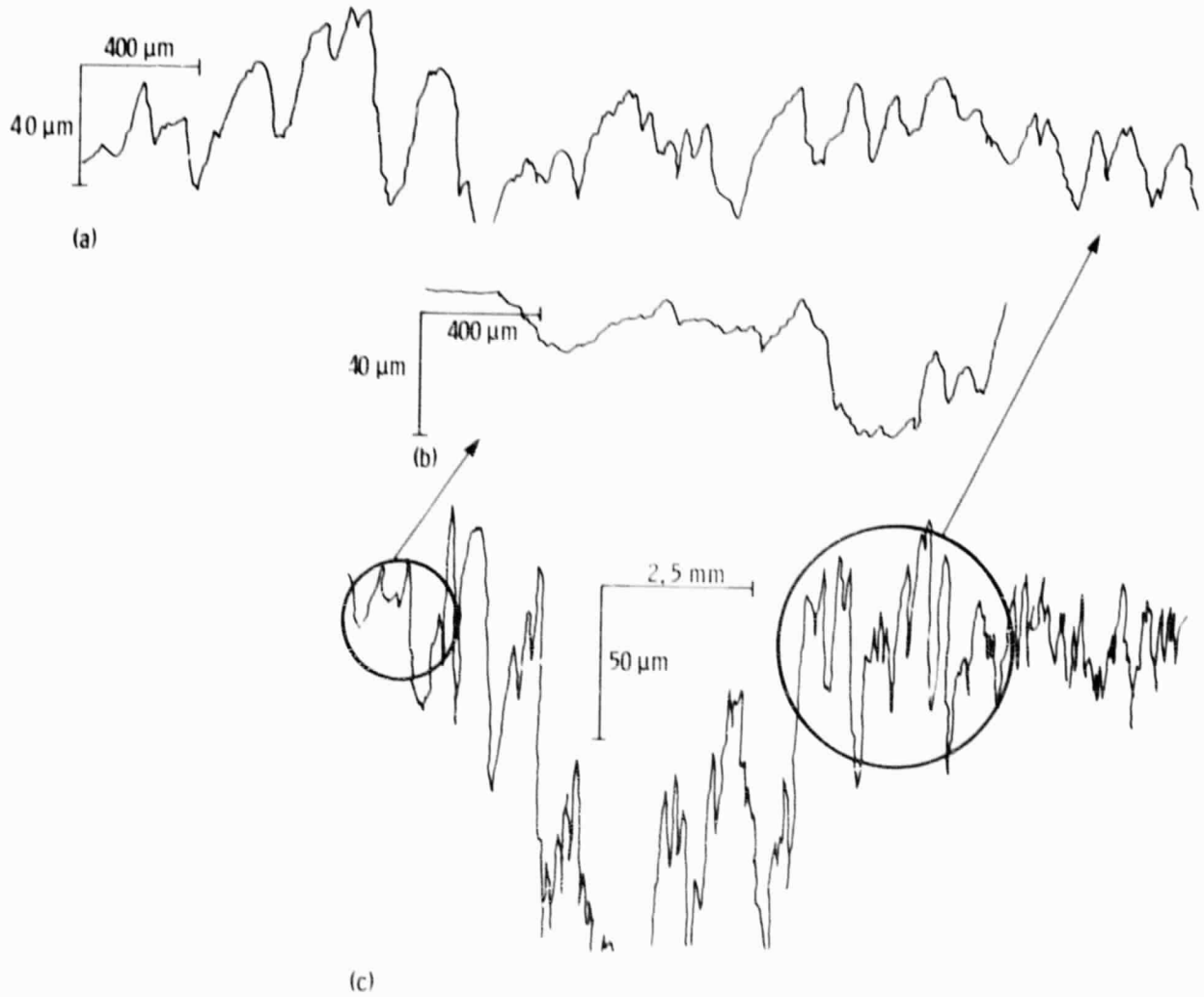

(a) Detailed profile.
(b) Detailed profile.
(c) Highly eroded region.

Figure 6. - Profiles on eroded surface along b-b as marked in figure 4(a).